

Tunable X-ray source based on mosaic crystals using for practical applications

This article has been downloaded from IOPscience. Please scroll down to see the full text article.

2010 J. Phys.: Conf. Ser. 236 012034

(<http://iopscience.iop.org/1742-6596/236/1/012034>)

View [the table of contents for this issue](#), or go to the [journal homepage](#) for more

Download details:

IP Address: 79.140.73.67

The article was downloaded on 06/07/2010 at 08:29

Please note that [terms and conditions apply](#).

Tunable X-ray source based on mosaic crystals using for practical applications

D A Baklanov, Duong Thi Giang, R A Shatokhin, I E Vnukov and Yu V Zhandarmov

Belgorod State University, 14 Studencheskaya str., Belgorod 308007, Russian Federation

E-mail: vnukov@bsu.edu.ru

Abstract. The prospect of creation of the X-ray source with tunable wavelength on the base of a middle energy accelerator and oriented crystals are analyzed. It is proved, that due to the contribution of diffracted bremsstrahlung, the mosaic crystals provide the essentially greater yield of hard radiation, than perfect crystals. The method of choosing crystals with necessary characteristics in contribution ratio of parametric X-ray and diffracted bremsstrahlung in radiation yield is proposed.

1. Introduction

Generation mechanisms of X-ray, appeared when fast charged particles interact with periodic structures, have been extensively studied in the past two decades [1]. The interest to this study is caused by the search for new tunable X-ray sources, capable to offer an alternative to storage rings. One of such mechanisms is parametric X-ray (PXR) of fast electrons in crystals [2, 3]. Advantages of PXR over other sources, based on the use of radiation of fast particles in substance, is the opportunity to vary the energy of photons by the change of orientation of a crystal or a position of the radiated object and smaller doze loadings as PXR is let out at the big angles to the direction of an electron beam. It is supposed that the most perspective is the use of this type of radiation in medical purposes, where small sources of hard quasimonochromatic X-ray ($\omega \geq 20$ keV, $\Delta\omega/\omega \leq 5\%$) [4, 5, 6] are demanded.

Measurements of the PXR characteristics, performed for a range of conventional crystals with perfect structure: diamond, silicon, germanium, tungsten, quartz, lithium fluoride (see [1] and references therein) showed that the radiation yield weakly depends on the crystal and is not enough for the practical realization of the source, based on this mechanism of radiation. The ways of radiation yield increase, offered recently (see, for example, [6, 7] and references therein) also hasn't found any practical application.

In works [8, 9] it is noted that the use of ideal mosaic crystals permits to increase significantly the radiation yield due to the contribution of diffracted photons of the bremsstrahlung (DB) or transition radiation (DTR). In quoted works the DB (DTR) contribution to the yield of the registered radiation in some times exceeded the PXR contribution and was well described by the theory of X-ray diffraction in mosaic crystals [10]. Accordance of the measuring results for the mosaic crystals of pyrolytic graphite [8] and diamond [9] with the calculation allows to compare perfect and mosaic crystals from the point of view of their use for generation of hard X-ray emission and appreciate possible advantages and disadvantages.

2. General expressions

As it is noted above mosaic crystals are able to provide higher intensity of quasimonochromatic radiation by means of additional contribution of DB and DTR mechanisms, than perfect crystals. However, as for these crystals PXR yield remains high, it is necessary to consider the contribution of this mechanism to the radiation observed. The kinematic PXR theory describes the measuring results with the fault not worse than 10-15% (see, for example, [11] and references therein), that is why to count the PXR yield the formula of spectral and angular distribution, obtained by the kinematical approach in the work [12] is used:

$$\frac{d^2N}{dZd\Omega} = \frac{\sum_{\nu} \alpha \omega^3 |\chi_{\vec{g}}|^2}{2\pi \epsilon_0^{3/2} \beta (1 - \sqrt{\epsilon_0} \vec{\beta} \vec{n})} \left[\frac{(\omega \vec{\beta} - \vec{g}) \vec{e}_{\vec{k}\nu}}{(\vec{k}_{\perp} + \vec{g}_{\perp})^2 + \frac{\omega^2}{\beta^2} \{\gamma^{-2} + \beta^2 (1 - \epsilon_0)\}} \right]^2 \quad (1)$$

Here and further the system of units used is $\hbar = m_e = c = 1$. Here $\epsilon_0 = 1 - \omega_p^2/\omega^2$, where ω_p - plasma frequency of medium, $\vec{\beta} = \beta \vec{n}_0$ - vector of electron speed, \vec{n}_0, \vec{n} - unit vectors in the line of the flying electron and emitted photon (with energy ω and momentum \vec{k}), \vec{g} is the reciprocal lattice vector, $\vec{e}_{\vec{k}\nu}$ are the polarization vectors, $\vec{e}_{\vec{k}1} = \frac{[\vec{n}, \vec{n}_0]}{|\vec{n}, \vec{n}_0|}$, $\vec{e}_{\vec{k}2} = [\vec{e}_{\vec{k}1}, \vec{n}]$, \perp - index, indicated the projections of vectors on the plane, which is parallel to \vec{n}_0 . The other notations are conventional. The term $|\chi_{\vec{g}}|^2$ denotes the following value:

$$|\chi_{\vec{g}}|^2 = |S(\vec{g})|^2 \exp(-2W) \left[-\frac{\omega_p^2}{\omega^2} \frac{f(\vec{g})}{z} \right]^2 \quad (2)$$

Here $|S(\vec{g})|^2$ is the structure factor, $\exp(-2W)$ is the Debye-Waller factor, $f(\vec{g})$ is the Fourier component of the spatial distribution of electrons in a crystal atom ($f(0) = z$, where z is the number of electrons in an atom).

As it is shown in [13] the total PXR yield doesn't depend on crystal mosaicity. During the radiation collimation mosaicity causes the broadening of the orientational dependencies (OD) and PXR angular distributions, and in case of comparability of Θ_{ph} and mosaicity factor σ_m it decreases radiation yield at the expense of PXR photons re-reflection [8]. The crystal mosaicity was taken into account by the calculation of the spectrum for different mosaic blocks, taking into account their distribution in the target.

It is known (see [10] and quoted literature) that by the perfection degree crystals can be classified by two factors: sizes of regular blocks or areas in a crystal and the extent of their mutual disorientation. According to the first factor all the crystals can be divided into to classes a and b . In the a class crystals separate areas are large enough for the primary extinction influence was visibly revealed, i.e. their linear size is comparable with the primary extinction length l_{ex} . In the class b crystals the regular block size is small that is why the effect of primary extinction is not observed. According to the second factor crystals also can be divided into two classes - α and β . In the α class crystals the blocks are almost parallel to each other, their mutual disorientation is small, that is why the contribution of the secondary extinction is big. In the class β crystals blocks are distributed irregularly, that is why the contribution of the secondary extinction is small.

Combining these factors we can classify crystals by their perfection degree into 4 groups from $a\alpha$ to $b\beta$. Class limit when possible disorientation of mosaic blocks is less than the area of total X-ray reflection (Darwin's table) is an ideal perfect crystal, and the class $b\beta$ limit is an ideal mosaic crystal. It should be noted that belonging to these classes isn't prescribed once and for all, as it depends on the extinction length, which in its turn depends on the order of reflection and photon energy [10].

It is known that the X-ray reflectivity of crystals is directly related to the perfection of their structure. Class $a\alpha$ crystals provide the least narrow rocking curve (FWHM ~ 20 - $30''$), which

is well described by dynamical theory of X-rays diffraction in perfect crystals. For this reason, their integral reflectivity is small. Crystals with a damaged structure have bigger reflectivity. Class $b\beta$ mosaic crystals have maximum reflectivity and the broadest rocking curve.

Class $a\alpha$ crystals can be represented sometimes as a set of crystallites, i.e. perfect crystals of small sizes, each of which reflects X-rays in accordance with the dynamic theory of diffraction. Reflectivity of such a crystal as a whole is close to the reflectivity of a perfect crystal with the same sizes, if the size of the crystallite is greater than the radiation absorption length. Otherwise, reflectivity of such crystal is bigger than of perfect one, since the radiation can be reflected from the crystallites located deeper in the course of the beam [10].

Characteristic parameters of the above classification of crystals - the width of the Darwin "table" $\Delta\Theta$ and the length of the primary extinction l_{ex} depend on the reflection order and photon energy [10]. For unpolarized radiation and the lack of absorption it can be written:

$$\Delta\Theta = 2 \cdot \gamma \Delta\theta_0, \quad (3)$$

where $\Delta\theta_0 = 2 \cdot \delta / \sin 2\Theta$ - allowance to the Bragg angle Θ because of the wave refraction in a crystal, $\delta = (\omega_p/\omega)^2/2$ - the difference of refraction index from 1, $\gamma = \frac{1}{2} \frac{F(\vec{g})}{F(0)} (1 + \cos(2\Theta))$, and $F(\vec{g}) = S(\vec{g})f(\vec{g})$ - a structure factor.

As an estimation of the primary extinction length one can use the expression:

$$l_{ex} = d / (2\bar{\xi} \sin \Theta), \quad (4)$$

where d - interplanar distance, and $\exp(-2\bar{\xi})$ - weakening of primary wave intensity when passing through one plane:

$$2\bar{\xi} = \frac{\pi d^2 N F(\vec{g})}{n} \frac{e^2}{mc^2}. \quad (5)$$

Here N is scattering centers concentration, n - the order of reflection.

If you use crystals to generate intense beams of X-ray a divergent photon beam with continuous spectrum falls on it or occurs in it, some of photons of which are then reflected and recorded by the detector with the fixed angular location. In such experimental set up the imperfect structure causes broadening of the detected radiation spectrum and its intensity increase. That is, for the a class $a\alpha$ crystal the detected radiation is of the least intense, and the spectrum width and orientational dependence is mainly determined by the radiation collimation angle ϑ_c . For the class $b\beta$ crystal radiation intensity is maximum and the width of the orientation dependence and the radiation spectrum are determined basically by the crystal mosaic structure.

The main advantage of mosaic crystals is the additional contribution to the registered spectrum of diffracted real photons. For the electrons of medium energy ($E_e \leq 100$ MeV) the main photon source is the bremsstrahlung (BS). For the relativistic electron and soft photons ($\omega \ll E_e$) the spectral and angular distribution of BS intensity produced per unit of path length in an amorphous substance can be represented in the form [14]:

$$\frac{d^2 I}{d\omega d\Omega} = \frac{\gamma^2}{\pi L} \frac{1 + \gamma^4 \theta^4}{(1 + \gamma^2 \theta^2)^4}, \quad (6)$$

where L is the radiation length, θ - angle of photon outlet.

In the analyzed case in the crystal the divergent photon beam with continuous spectrum occurs. To reflect a monodirect and monochromatic photon beam with the energy ω and direction \vec{n} from the element of mosaic crystal with volume ΔV can be wrote as [10]:

$$\int P(\theta) d\theta = Q \Delta V, \quad (7)$$

where $P(\theta)$ - reflecting power of the crystal element at the angle θ , which is proportionate to the distribution of mosaic blocks in the crystal [15]. $Q\Delta V$ - integral reflection from the element ΔV , Q - the X-ray reflectivity depends on the crystal parameters and the radiation energy as:

$$Q = \left(\frac{e^2}{mc^2} \right)^2 \frac{N^2 \lambda^3}{\sin(2\Theta)} |F_p| |F(\vec{g})|^2 \cdot \exp(-2W), \quad (8)$$

where λ - wavelength, $|F_p|$ - polarization multiplier. For an unpolarized photon beam $|F_p| = (1 + \cos^2 2\Theta)/2$.

Let the radiation with the spectral and angular intensity distribution $I(\omega, \vec{n})$ be spread in a mosaic crystal possessing the distribution of reciprocal lattice vectors $P(\vec{g})$. Here $\vec{g} = |\vec{g}|\vec{\alpha}$, where $\vec{\alpha}$ is the unit vector specifying the deflection of crystal mosaic blocks from the average direction $\vec{g}_0 = \langle \vec{g} \rangle$. Starting from Bragg law for the photon with energy ω and direction \vec{n} we can obtain the direction of vector \vec{g} of the block, on which this photon can diffract, and the driving direction of the reflected photon \vec{n}' . Then probability density of the reflection of photon with fixed ω and \vec{n} in the block of mosaic crystal with the thickness Δt along the photon driving direction can be written as:

$$f(\omega, \vec{n}) = q(\omega, \vec{n})Q(\omega)\Delta t, \quad (9)$$

where $q(\omega, \vec{n})$ - a factor of the crystal mosaicity:

$$q(\omega, \vec{n}) = \int P_m(\alpha_x(\omega, \vec{n}, \alpha_y), \alpha_y) d\alpha_y. \quad (10)$$

Here $P_m(\alpha_x, \alpha_y)$ - distribution of crystal mosaicity, expressed through $\omega, \vec{n}, \alpha_y$ [8].

To calculate the yield of the diffracted photons in the aperture of the collimator for each order of the reflection i , spectral and angular distribution of the radiation intensity, taking into account multiple electron scattering in the target $\frac{d^2 I(\omega, \vec{n})^*}{d\omega d\Omega}$, was reduced with the probability density of the diffraction by all variables, including energy, angles of photon outlet θ_x and θ_y and the crystal thickness T :

$$Y_i = \int_{\Delta\omega_i} d\omega \int_T dt \iint_{\Delta\Omega} \frac{d^2 I(\omega, \vec{n})^*}{d\omega d\Omega} S(\omega, \vec{n}, \vec{n}', t) Q(\omega) q(\omega, \vec{n}) d\theta_x d\theta_y, \quad (11)$$

here $S(\omega, \vec{n}, \vec{n}', t)$ - factor considering the radiation absorption in the target material and the experiment geometry, $\Delta\Omega$ angular acceptance, and $\Delta\omega_i$ energetic capture of the detector for i reflection order.

According to the kinematic PXR theory for the definitely Bragg direction the intensity of radiation is equal to zero [2, 3, 12]. That is why in perfect crystals diffraction of PXR photons usually is not viewed. In mosaic crystals for the photon, produced in one of the mosaic blocks, the diffraction conditions in other block can be fulfilled. To consider this effect for each PXR photon with the energy ω and momentum \vec{k} from Bragg law in accordance with (9)-(10) the blocks of mosaic, on which this photon can diffract, and the probability of reflection were defined. From here, taking into account the distribution of the mosaic blocks, PXR photon beam attenuation on its way from the birth point to the outlet out of crystal was defined. More detailed the method of calculation of the PXR and DB yields in the mosaic crystals was described in [8].

3. Comparison perfect and mosaic crystals

The PXR yield linearly depends on the thickness of the crystal, that is why the natural way to increase the intensity is to enlarge the thickness of a target. In Figure 1 there is a calculated dependence of PXR yield for the reflection (220) and $\Theta_B = \Theta_D/2$ from the thickness of the

silicon crystal for the following conditions: $E_e=45$ MeV; electron beam divergence $\vartheta_e=1.5$ mrad; observation angle $\Theta_D=16.7^\circ$ ($\omega \sim 33$ keV); $\vartheta_c = 0.85$ mrad.

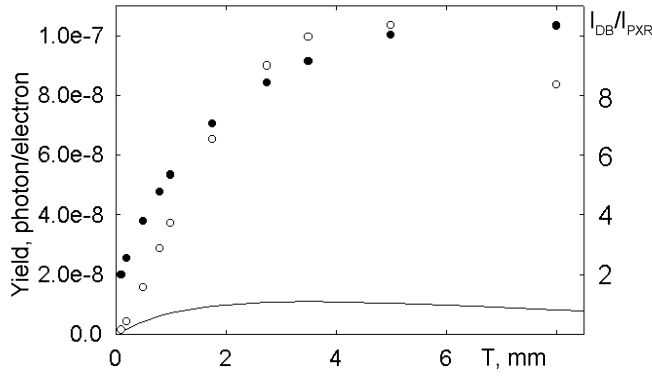


Figure 1. The dependence of PXR and DB intensity on the silicon crystal thickness. Curve - PXR, \circ - DB, \bullet - Y_{DB}/Y_{PXR}

The use of class *b* mosaic crystals permit to get essentially bigger radiation yield due to the DB contribution [8, 9]. In this figure there is also a dependence of DB yield for the mosaic sample with $\sigma_m=1$ mrad (circles) and the ratio of DB and PXR yields (points). It is clear from the figure that even for $T=0.1$ mm the DB yield from the mosaic crystal is bigger than the PXR yield from perfect one. As the PXR yield little depends on the sample mosaicity [13], and the DB yield from the perfect crystal is less than PXR yield [16], a mosaic crystal almost always provides the bigger radiation yield than perfect one. It should be noted that fulfilling the condition $\sigma_m < \vartheta_c$ the DB spectrum is narrower than PXR spectrum [9], e.g. for $\sigma_m=0.6$ mrad and $T=3.5$ mm the full width of the spectrum (on level 10% from max) $\Delta\omega_{DB}=1.2$ keV is less than for the PXR spectrum $\Delta\omega_{PXR}=1.95$ keV, and the relation of intensities ~ 8 .

As it is seen from the figure, the maximum of the PXR and DB yield is reached for the crystal thickness is about the absorption length of photons. That is why with the decrease of the photon energy the advantage of the mosaic crystals over perfect ones becomes lesser. E. g. for $E_e=45$ MeV, of a silicon crystal and photon energy $\omega \approx 18$ keV the relation of the DB and PXR yields for the target with optimal thickness decreased to ~ 4 [8].

The main problem when we use the crystals with optimal thickness to generate radiation is not the spectrum width but the big BS background in the location of the radiated object. As was shown in Ref.[17] the number of BS and DB photons, fallen on the radiated object when using the crystals of optimal thickness, as a rule is comparable and the full energy is in some extent bigger than the full energy of useful radiation. Apparently this is the main reason why the authors' idea [5] about using PXR beam from a thick pyrolytic graphite crystal for mammography was not realized.

One of the solutions for this problem is a double-crystal scheme. Recently in the work [18] the system of two perfect crystals for the PXR generation in a thin crystal and its subsequent diffraction in another, thicker one was realized. The main advantage of such scheme is that the narrow width of spectrum leads to low radiation intensity. If the width of the spectrum is not a critical parameter, e.g. for the radiography, where $\Delta\omega/\omega \sim 2-3\%$ may be enough, than the use of mosaic crystals instead of the perfect ones can essentially enlarge the radiation yield [9].

To realize the merits of mosaic crystals for the obtaining of intensive X-rays the samples with low *Z* and $\sigma_m < 0.4-0.6$ mrad are necessary. The low limit of σ_m and the required sizes of blocks are determined by the limits of the application of the class *b* mosaic crystal model $\sigma_m \gg \Delta\Theta$ and $l \ll l_{ex}$. These crystals can be used on the beams of synchrotron radiation instead of perfect crystals with asymmetric cut or curved ones [19], when high intensity is demanded and there are no strict requirements for its monochromaticity.

4. Choice of crystals

For most applications, which require high monochromaticity of radiation, the use of pyrolytic graphite crystals is limited because of the large value of mosaicity factor. As shown above, and in the work [9], the other crystals, which meet the requirement that $\sigma_m \gg \Delta\Theta$ and $l \ll l_{ex}$ should have the same merits. The choice of crystals with small mosaicity is easily done with the help of conventional methods of X-ray analysis. Estimation of mosaic blocks sizes and the angles of their relative misalignment is a more complex experimental task, which is successfully solved by conventional methods only for the surface layers, for example, see [20].

Characteristic parameters of the classification $\Delta\Theta$ and l_{ex} depend on the reflection order and photon energy. In this regard, we analyze the measuring results for significantly different photon energies. Figure 2 shows the measuring results of the vertical angular distribution of radiation yield for the reflection (220) from the crystal of a natural diamond with the sizes $6 \times 10 \times 0.35$ mm³ in the experiment [21] (circles) for the following experimental conditions: $E_e=900$ MeV, $\Theta_D=90^\circ$, $\vartheta_c=1.88$ mrad, $\sigma_m \approx 0.2$ mrad. The crystal is installed in Bragg geometry ($\Theta_B=45^\circ$) so, that the thickness of the target along the electron beam was ≈ 0.5 mm.

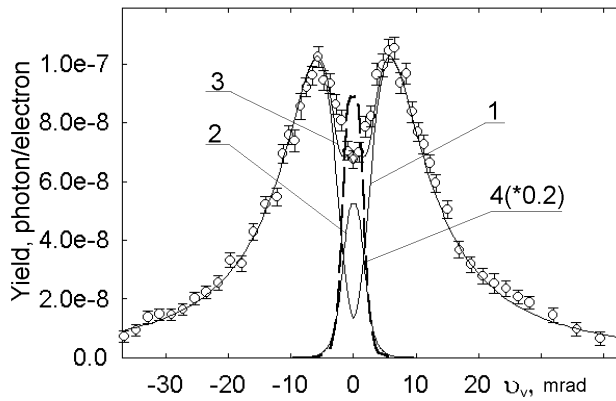


Figure 2. The vertical angular distribution for the experiment [21]. \circ - experiment. Lines - calculation: 1- PXR for the perfect crystal; 2 - DTR for the perfect crystal; 3- PXR+DTR for the perfect crystal; 4 - DTR for the class $b\beta$ mosaic crystal.

Dependence 1 in this figure is calculation results according to the kinematic PXR theory [12] in the assumption that the crystal is perfect. As it is shown in the works [8, 9, ?], under the condition $\sigma_m \ll \Theta_{ph}$, as in this case, mosaicity has almost no effect on the spectrum and angular PXR distribution. As in the quoted experimental work, because of the normalization fault (~ 20 - 30%) measurements are normalized to the calculation results of photons emission angle $\vartheta_v \geq 5$ mrad. The figure shows that the calculated dependence soundly describes the experimental results only for the angles $\vartheta_v \geq 5$ - 7 mrad. For smaller angles the experimental points are significantly higher than the calculated curve, indicating the contribution of radiation with narrower angular distribution than PXR, i.e. the contribution of real photons diffraction. In this case ($\omega \sim 6.97$ keV $\ll \gamma\omega_p \sim 67$ keV) it is DTR.

Curve 2 shows the results of the calculation of vertical dependence of DTR yield carried out according to the method of work [22]. Curve 3 is the resulting angular distribution of PXR + DTR, which satisfactorily describes the experimental results. Nevertheless, in the center of the angular distribution experimental and calculated dependencies are somewhat different, which is apparently caused by a crystal mosaicity (see below).

Mosaicity factor $\sigma_m \sim 0.2$ mrad is comparable with the width of total reflection area for this photon energy $\Delta\Theta \sim 0.02$ mrad. Therefore, by the degree of blocks disorientation this crystal should be attributed to class α . To test the applicability of a mosaic class b crystal approach to this model, the angular DTR distribution in this approximation by the method of the work [22](curve 4) was calculated. It is seen from this figure that the angular DTR distribution for the perfect and mosaic crystals are similar, but differ in intensity almost by an order of magnitude.

Curve 3 is closer to the experimental points than the sum of curves 2 and 4, therefore the diamond crystal, used in the experiment [21], should be classified as $a\alpha$ class, i.e. the sizes of its constituent crystallites are greater than $l_{ex} \sim 7 \mu\text{m}$. The difference between curve 3 and the experimental results is caused by the fact that for photons with $\omega = 6.97 \text{ keV}$, the absorption length $l_a \sim 0.43 \text{ mm} \gg l_{ex}$. Therefore blocks, located in the depths of the crystal and disoriented relative to the blocks on the surface $\Delta\Theta$, can contribute to the detected radiation yield. The value of this contribution is very small in comparison with a ratio of values σ_m and $\Delta\Theta$ (see above and Fig. 2), therefore, the crystallite size is significantly bigger l_{ex} .

In Figure 3 the points show the dependence of the first order reflection photons yield from the angle of (110) plane misalignments relative to the direction of Bragg reflection obtained in the experiment [9].

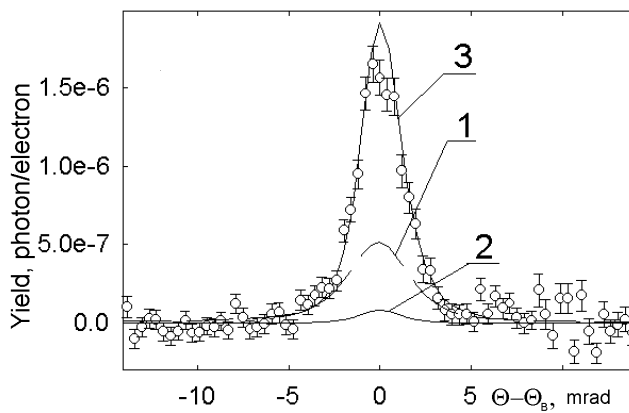


Figure 3. The orientation dependence for the experiment [9]. \circ - experiment. Lines - calculation: 1- PXR for the perfect crystal; 2 - DB for the perfect crystal; 3- PXR+DTR for for the class $b\beta$ mosaic crystal.

Experiment is made in Laue geometry on the natural diamond crystal with the surface mosaicity $\sigma_m \sim 0.2 \text{ mrad}$, the orientation of $\langle 110 \rangle$, and sizes $6 \times 8 \times 2 \text{ mm}^3$, cut from the same sample as the target, used in the experiment [21]. Experimental conditions: $E_e = 500 \text{ MeV}$, $\Theta_D = 4^\circ$ ($\omega \sim 145 \text{ keV}$), $\vartheta_c = 1.9 \text{ mrad}$.

Curve 1 shows the calculated dependence obtained within kinematic PXR theory. Measured and calculated OD are close enough in form, but differ significantly in amplitude. The difference in the widths (FWHM) of calculated and measured dependencies $\Delta\Theta_{calc} = 3.97 \text{ mrad}$ and $\Delta\Theta_{exp} = (2.9 \pm 0.2) \text{ mrad}$ exceeds the experimental fault (measurement pitch OD $\approx 0.4 \text{ mrad}$) and witnesses the radiation contribution with a narrower angular distribution than PXR. For the conditions of the quoted work ($\omega \approx 145 \text{ keV} \gg \gamma\omega_p \sim 35 \text{ keV}$) it is DB.

Evaluation of DB contribution by the method of the Ref. [16] in the assumption, that the crystal is perfect, (curve 2) showed that in this case DB yield does not exceed 25% of the PXR one and cannot explain the experimental results. Accounting of the crystal mosaicity by the method [8] in the assumption of a homogeneous distribution of mosaic blocks with sizes smaller than the primary extinction length $l_{ex} = 148 \mu\text{m}$ in the crystal thickness, i.e. its belonging to the mosaic crystals of class $b\alpha$, showed that the difference is indeed caused by mosaicity. The resulting dependence of PXR+DB, calculated with due account for the mosaicity for both components (curve 3) is close to the experimental one. The calculated values of the yield $Y_{calc} = 1.94 \cdot 10^{-6} \text{ phot./electr.}$ and the width of the OD of $\Delta\Theta_{calc} = 2.67 \text{ mrad}$ are satisfactory agreed to the measuring results $Y_{exp} = (1.63 \pm 0.008) \cdot 10^{-6} \text{ phot./electr.}$ $\Delta\Theta_{exp} = (2.9 \pm 0.2) \text{ mrad}$ [9].

Both targets are cut from the same sample of natural diamond. Consequently, their microstructure has to be approximately the same. However, the measurements for them are described in different models. For $\Theta_D = 90^\circ$ the crystal appears as a perfect or $a\alpha$ class mosaic crystal. For $\Theta_D = 4^\circ$ the results are described in the approximation of $b\alpha$ class mosaic crystal.

Different manifestations of the same crystal structure is caused by the energy difference of the

detected radiation. With photon energy increasing l_{ex} increases and $\Delta\Theta$ decreases. Therefore, with photon energy increasing any imperfect crystal becomes a class b mosaic crystal. That is, changing the observation angle one can trace the transition from one description to another, and, therefore, estimate the sizes of mosaic blocks. PXR theory in the kinematic approximation describes the results of measurements carried out in the perfect crystals with an error not worse than 10-15% [11]. With same accuracy the theory of X-ray diffraction in mosaic crystals describes the yield of DB and DTR from class b mosaic crystals [8]. Therefore having measured the radiation yield at Bragg angles for several observation angles and compared it with the predictions of the kinematic PXR theory one can register a contribution of real photon diffraction and make a conclusion about the average sizes of blocks which form the sample.

These values behave this way with of the reflection order increasing. Consequently, having measured the angular distribution of radiation for one observation angle and different orders of reflection, and compared it with the calculation results of PXR and DB+DTR yields for the perfect crystal and the mosaic class b crystal, we can determine for which reflection order the transition from one description to another will start, i.e. to estimate the average size of blocks.

5. Conclusion

The results of the conducted researches can be formulated in the following way:

1) Use of the class $b\beta$ mosaic crystals instead of the perfect ones in a great extent increases the quasimonochromatic X-radiation yield. Mosaicity $\sigma_m < \vartheta_c$ provides the increasing of the radiation yield without noticeable worsening of radiation monochromaticity.

2) Registration of the radiation yield at Bragg angles (DTR+PXR+DB) for different observation angles (different reflection orders) permit to obtain the information about characteristic sizes of blocks, which form the test sample, and its applicability for getting intensive beams of quasimonochromatic X-ray.

This work is supported in part by the internal grant of Belgorod State University.

References

- [1] Rullhusen R, Artru X and Dhez P 1999 *Novel Radiation Sources Using Relativistic Electrons* (Singapore: World Scientific)
- [2] Garibian G Shi Yang 1971 *Sov. Phys. JETP* **61** 930
- [3] Baryshevskii V, Feranchuk I 1971 *Sov. Phys. JETP* **61** 944
- [4] Baldelli P, Taibi A, Tuffanelli A, Gambaccini M 2004 *Physics in Medicine and Biology* **49** 4125
- [5] Peistrup M A *et al* 2001 *Review of Scientific Instruments* **72** 2159
- [6] Takashima Y *et al* 1998 *NIM B* **145** 25
- [7] Kaplin V V *et al* 2002 *Applied Physics Letters* **80** 3427
- [8] Bogomazova E A *et al* 2003 *NIM B* **201** 276
- [9] Baldin A N, Vnukov I E, Shatokhin R A 2007 *Technical Physics Letters* **33** 625
- [10] James R *The optical principles of the diffraction of X-rays* 1958 (London: G. Bell and Sons)
- [11] Brenzinger K-H *et al* 1997 *Phys. Rev. Lett.* **79** 2462
- [12] Nitta H 1991 *Phys. Lett. A* **158** 270
- [13] Afanas'ev A M and Aginian M A 1978 *Sov. Phys. JETP* **74** 300
- [14] Bazylev V A, Zhevago N K *Radiation of Relativistic Particles in External Fields and in Matter* 1987 (Moscow: Nauka Pub.) (in Russian).
- [15] Chabot M *et al* 1991 *NIM B* **61** 377
- [16] Baklanov D A, Baldin A N, Vnukov I E, Nechaenko D A, Shatokhin R A 2007 *The Journals of Kharkiv National University* **763** No.1(33) 41 (in Russian)
- [17] Shatokhin R A, Vnukov I E, Zhandarmov Yu V 2009 *Problems of Atomic Science and Tekhnology, Series "Nuclear Physics Investigatios"* **51** 113
- [18] Hayakawa Y *et al* 2006 *NIM B* **252** 102
- [19] Arfelli F 2000 *NIM A* **454** 11
- [20] Ohler M, Baruchel J, Moore A W, Galez Ph, Freund A 1997 *NIM B* **129** 257
- [21] Baldin A N, Vnukov I E, Kalinin B N, Karataeva E A 2006 *Poverkhnost'* No. 4, 72 (in Russian)
- [22] Adischev Y N *et al* 2003 *NIM B* **201** 114